NOVEL APPLICATIONS OF OPTICAL DIAGNOSTICS

O. Chubar, ESRF, Grenoble, France

Abstract

New methods of optical diagnostics and improvements in existing techniques based on synchrotron radiation (SR) are discussed. The review covers recent advances in electron beam imaging with use of new instruments (such as refractive lenses for X-rays) and more efficient exploitation of wave-optics features of synchrotron light. SR interference techniques - to measure the transverse size of electron beam - and new projection methods - to characterize the beam angular divergence - are considered. Practical examples of the electron beam emittance measurements using the SR of the X-ray and visible spectral range are presented.

1 INTRODUCTION

Optical methods have proved to be very efficient for diagnostics of relativistic charged particle beams emitting synchrotron radiation in magnetic fields of accelerators.

In third-generation SR sources, the RMS transverse size of the emitting beam can be as small as ~10 μm, and the angular divergence on the order of several micro-radians. The measurement of these small values is the challenging goal for today's optical diagnostics. This goal motivates the developments of new high-resolution techniques.

The principles of the optical diagnostics are very simple. The emitted radiation "inherits" the information on particle distribution from the electron beam. In a few cases, this information can be "extracted" by straightforward optical measurements. The use of high-accuracy wave-optics calculations of the SR emission and propagation increases the number of experimental schemes and types of radiation that can be successfully applied for the beam diagnostics. In particular, it allows using those emission and observation schemes that are intrinsically very sensitive to the parameters of the emitting beam, yet requiring more thorough theoretical interpretation of the measured results.

Formally, the optical methods can be classified according to their wavelength range. On the other hand, the progress in X-ray optics during the last years was so significant, that the same methods are now used both with visible light and X-rays. Therefore, during the discussion, we will try to group methods mainly based on their physical content.

2 ADVANCES IN BEAM IMAGING

The traditional use of the imaging technique is to obtain a high-quality SR focusing, such that the spot size produced by one electron is much smaller than the size of the electron beam (assuming 1:1 imaging). Once this is met, the measured intensity distribution can be treated as a transverse distribution of particle density in the beam.

In third-generation SR sources, the optical resolution at the traditional beam imaging with visible light [1-3] is not sufficient for the measurement of a small vertical beam size [4,5]. The following two sub-sections illustrate two different approaches to improve the resolution: the use of the imaging schemes with X-rays and better exploitation of the SR wave-optics features.

2.1 New and Existing X-ray Focusing Tools

The arsenal of X-ray focusing tools was recently enriched by refractive lenses [6-9]. The first refractive X-ray lenses were fabricated by drilling a number of well-aligned holes in aluminium or beryllium. The material between the holes focuses the incident X-rays (see Fig. 1). Due to the large number of holes used typically, these devices are called **compound refractive lenses** (CRLs).

To discuss the features of CRL, let us recall that the real part of the refractive index n is very close to unity for X-rays in most materials. For beryllium and aluminium at 20 keV photon energy (λ = 0.62 Å), the refractive index decrement δ ($\delta \equiv n - 1$) is, respectively: 8.5×10^{-7} and 1.35×10^{-6} [10].

The focal distance of a compound refractive lens composed of an array of N holes is estimated as [6]:

$$F \approx R/(2N\delta), \qquad (1)$$

where R is the radius of curvature of the focusing surface. A focal distance of 10 m can be obtained, for example, at N = 10 and the radii of curvature as small as $r \approx 170$ μm (Be) and $r \approx 270$ μm (Al).

The optimal shape for a focusing surface is known to be a paraboloid, because it only modifies the quadratic terms of the radiation phase (essential for focusing), with no extra aberrations. For CRLs, the effect of using the parabolic surfaces instead of the circular ones is very pronounced, because their surface curvature radius is comparable with the aperture size [9].

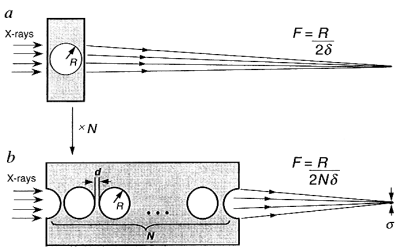

Figure 1. The principles of X-ray focusing by a CRL [6].

In spite of the small wavelengths at which they operate (~0.2 to ~2 Å), the CRLs have moderate surface quality requirements. The phase error $\Delta\Phi$ due to deviation Δs of one focusing surface from the ideal shape is:

$$\Delta\Phi \approx 2\pi\ \Delta s\delta/\lambda\,, \qquad (2)$$

i.e., if $\lambda = 0.62$ Å and $\delta = 8.5\times10^{-7}$, a requirement $|\Delta\Phi| < 1$ is satisfied at $|\Delta s| < 11.6\mu m$ (!). In view of possible use of many individual lenses in a CRL, one would need better surface quality than estimated above; nevertheless, the required quality seems well obtainable with the existing CRL manufacturing technology [9].

The CRLs were successfully applied for the electron beam size and transverse profile measurements [11,12]. At 23 keV photon energy, an aluminium parabolic CRL (0.9 mm geometrical aperture, 190 μm min. radius of surface curvature) located at 40 m from an undulator source, provides the optical resolution of ~4 μm [11]. This high resolution allows using the CRL for the electron beam size and profile measurement directly, with no need for sophisticated experimental data processing.

A CRL has an effective aperture due to absorption [7]. One way to increase the effective aperture is to use low-absorption material [7]. Another approach is to apply radial segmentation of the lens by rings, preserving the parabolic surface shape and removing the extra thickness of material (that produces the phase shift of integer number of 2π) from each ring. This makes the CRLs similar to **zone plates** with parabolic zone profile [9].

Due to strong dependence of the refractive index decrement on the wavelength [6,7], a monochromator or spectrum analyser has to be used with the CRLs and zone plates at the electron beam size or profile measurements.

Considerable progress was made in the quality of **curved mirrors** for X-ray focusing. The high-quality mirrors allow to measure the RMS electron beam size of ~20 μm [12]. The resolution is still limited by aberrations in this case.

The new X-ray tools do not replace the existing well-proven techniques. At ESRF, the **pinhole camera** is successfully used for the transverse beam size and profile measurements [13]. The pinhole camera allows to measure an RMS vertical beam size as small as ~13 μm (with equal contribution from the RMS size of transfer function). Among the advantages of the pinhole camera, one can mention: the possibility of carrying out measurements using the "white" SR from a bending magnet without a monochromator, insensitivity to heat load and high practical reliability.

2.2 Exploitation of SR Wave-Optics Features

The use of a small radiation wavelength is not the only approach to improve the resolution at the beam size measurements. Another possibility is to exploit the wave-optics features of the synchrotron radiation used for the imaging. An example of this approach is the use of the **vertical polarization** component of the bending magnet SR for the measurements of a small vertical size of electron beam [14].

Typical intensity distributions of the two different polarization components of the focused bending magnet SR are shown in Fig. 2 for a "filament" electron beam and for a beam with non-zero transverse size. Due to anti-symmetry of the vertical component of the SR electric field with respect to the horizontal median plane, the main peak of intensity distribution of the vertically polarized focused SR is split in the vertical direction, so that for the "filament" electron beam (or single electron), one would observe a zero intensity in the median plane. For a beam with non-zero transverse size, the intensity of the vertically polarized SR differs from zero in the median plane due to some broadening of the two off-axis peaks (Fig. 2-b, right). If the emitted SR is almost diffraction-limited, this effect is easier to observe experimentally, than a small broadening of the main peak of the horizontal polarization component (Fig. 2-a, right), as measured with the traditional electron beam imaging [2,3].

The measurements of the focused vertical polarization component of the visible-range SR, and the wave-optics calculations of the SR focusing, allowed to determine the RMS vertical size of the electron beam as small as 15 μm in a bending magnet of the MAX-II ring [14].

For this type of diagnostics to work well, it is important to use wave-optics methods and computer codes for the SR emission and propagation calculations. A few such codes are available now [15-18]. Once the calculations of the focused SR can be done, the transverse size of the emitting electron beam is obtained by fitting the measured intensity distributions in assumption of Gaussian particle distribution in the electron beam.

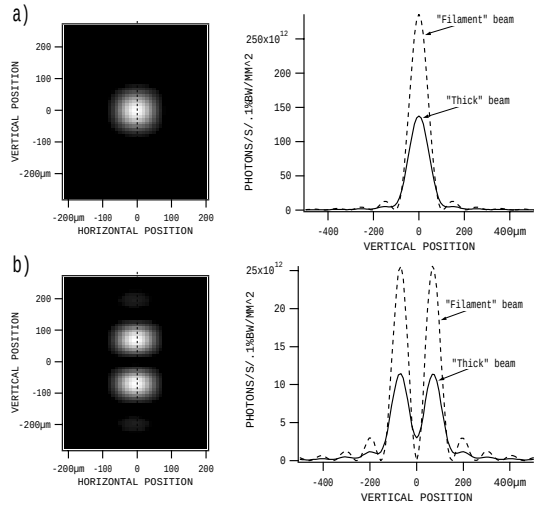

Figure 2. Intensity distributions of the focused bending magnet SR in the plane of 1:1 imaging: a) horizontal, b) vertical polarization component. Left: 2-d distributions for a "filament" electron beam; right: vertical intensity profiles for a "filament" and a "thick" beam.

At a somewhat more general approach, one can apply reconstruction of the electron beam profile from the measured 2D intensity distribution of the focused SR. The reconstruction consists in solving an integral equation of the first kind [19]. In [20], a similar approach was used to "subtract" the aberration due to thermal deformation of the first mirror, from the measured image of the electron beam profile.

3 INTERFERENCE METHODS

The measurement of transverse coherence of synchrotron radiation is another technique to determine the transverse size of the emitting beam. A number of optical methods based on the measurements of SR transverse coherence were suggested over the last few years both in visible [21-26] and X-ray range [27,28].

In these methods, one measures the visibility of fringes on a detector screen after the synchrotron radiation (e.g. from a bending magnet) passes through an interference scheme. If the transverse size of the emitting beam were zero, the visibility of the interference fringes would be unity in the transverse direction. Due to the non-zero size of the emitting beam, the visibility of fringes decreases. For example, in the simplest **"Lloyd's Mirror"** scheme, for the electron beam with Gaussian transverse distribution of particles (emitting incoherently), the interference fringes are modulated transversely by a Gaussian with the RMS size given by [21]:

$$\sigma_{\perp}^{*} = \frac{r\lambda}{4\pi(\sigma_{\perp}^{2} + h_{\perp}^{2}\sigma_{\lambda}^{2}/\lambda^{2})^{1/2}}, \qquad (3)$$

where r is the distance from the emission region to the observation plane, λ the radiation wavelength, σ_{λ} the RMS radiation bandwidth, $h_{\perp}$ the distance from the mirror plane to the electron beam, $\sigma_{\perp}$ the transverse size of the emitting beam ($\sigma_{\perp} << h_{\perp}$). Depending on the geometry of the interference scheme, the "$\perp$" index means a horizontal or vertical direction. We note that the intensity distribution after an interference scheme does not depend on angular divergence of the electron beam.[1]

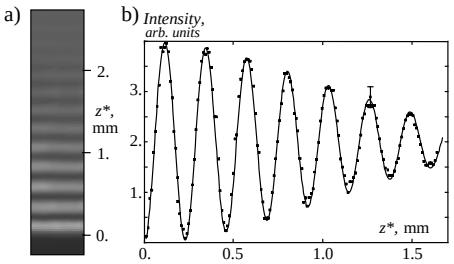

Figure 3. Interference pattern in the case of the horizontal mirror: a) fringes registered by CCD-camera; b) vertical intensity cut: measured and computed [22].

[1] This can be shown analytically, and is also understandable qualitatively, since with standard schemes, the interference is well observed for isotropic sources [29].

In line with Eq. (3), if one measures the visibility of fringes at some transverse position, one can determine the transverse size of the emitting beam. We emphasize the necessity of monochromatization, since a finite radiation bandwidth results in the same effect as the beam size, (see Eq. (3)). An example of SR intensity measured using the "Lloyd's Mirror" scheme is shown in Fig. 3. At MAX-II, a modification of this scheme allowed to measure the RMS vertical beam size of 22 ± 9 μm [5].

For a small transverse size of the emitting beam, the visibility of fringes is close to unity at a considerable transverse offset from the symmetry plane, and a straightforward use of the simplest interference scheme is not an optimum. A number of successful applications of more sophisticated visible-range **SR interferometers** for the measurements of the transverse size and profile of electron beam, with the resolution of several micrometers, were reported in [23,25,26]. A considerably higher resolution, up to several nanometers (!), was reached at SLAC using the **laser interferometry** method, where a laser beam was crossing the particle beam in 90º Compton scattering geometry [30]. One should mention the higher experimental complexity of these measurements.

A number of **X-ray interference** schemes were recently realized in practice [27,28]. As one of the most suitable for electron beam size measurements, the scheme with the boron fiber [28] can be mentioned. In this scheme, a thin fiber is used to split the SR wavefront and to produce an interference pattern on a detector screen.

The patterns created by the **Fresnel diffraction** at an edge or a slit can also be used as a source of information about the transverse size of the emitting beam [31]. A peculiarity of this method is that the visibility of diffraction fringes differs from unity even for a zero size of the emitting beam, therefore a high-accuracy measurements and simulations are necessary to extract the beam size value.

4 PROJECTION METHODS

Unlike the imaging and interference methods, which are sensitive to the transverse size, projection methods "feel" well the angular divergence of the emitting beam. Formally, both in the imaging and projection methods, the measured intensity distribution depends on the beam size that is propagated (using the rules of second-order moments propagation) from the emission region to the observation plane. However, in projection methods, the propagated size is no longer the de-magnified size of the particle beam. With no focusing optics in the emission region, the squared propagated RMS size is

$$\sigma_{x(z)\,eff}^{2} = \sigma_{x(z)}^{2} + 2M_{xx'(zz')}r + \sigma_{x'(z')}^{2}r^{2} \qquad (4)$$

where $\sigma_{x(z)}$ is the horizontal (vertical) RMS size of the beam, $\sigma_{x'(z')}$ its angular divergence, $M_{xx'(zz')}$ mixed second-order central moment: $M_{xx'} \equiv <(x-<x>)(x'-<x'>)>$; r is distance from the emission region to the observation

plane. At large r, the propagated size is $\sigma_{x(z)eff} \approx \sigma_{x'(z')} r$, i.e. the intensity distribution becomes only sensitive to the angular divergence of the emitting beam.

Finite electron beam divergence and size flatten the SR distribution that one would observe for a single electron. To be able to deduce the $\sigma_{x(z)eff}$ from a measured SR distribution, one needs the characteristic details of the single-electron distribution to be comparable to the $\sigma_{x(z)eff}$.

In third-generation SR sources, a natural choice for projection diagnostics can be **undulator** radiation (UR) [32-34]. At ESRF, the UR was used for several years as a primary emittance measurement tool [32]. In low-coupling mode, the vertical divergence of the electron beam can be smaller than the angular size of the central cone of single-electron UR even for X-rays. However, it is still larger than the angular width of an off-axis "undulator ring" [12,16]. Due to near-field effects in the off-axis UR [35], one needs to use a near-field calculation method to deduce the propagated beam size from intensity distribution in the "undulator ring".

Undulator spectrum vs. photon energy provides another possibility for beam diagnostics. The UR harmonic shape depends not only on the beam divergence and size, but also on its energy spread, with the two effects being well separable. This gives a possibility for the direct energy spread measurements [36]. A very high sensitivity to the beam energy spread and divergence is inherent to the **optical klystron** spontaneous spectra vs energy [37].

Besides UR, for the projection diagnostics, one can make use of **edge radiation** (ER), i.e. the radiation emitted at the edges of bending magnets bounding a straight section in a storage ring [38-43]. At wavelengths much larger than the critical wavelength value of the bending magnet SR, the spectral-angular distribution of the interfering ER emitted by one electron at two bending magnet edges, can be approximated (in the far field) as

$$\frac{dN}{dtd\Omega(d\lambda/\lambda)} \approx \frac{4\alpha I}{\pi^2 e} \frac{\gamma^4\theta^2 \sin^2[\pi L(1+\gamma^2\theta^2)/(2\lambda\gamma^2)]}{(1+\gamma^2\theta^2)^2}, \quad (5)$$

where α is the fine-structure constant, e the charge of electron, I the electron current, γ the reduced electron energy, θ the observation angle with respect to the straight section axis, L the straight section length. From Eq. (5), an estimation of angular width of the k-th interference ring (starting from the pattern center) is, at k>>1:

$$\Delta\theta_k \approx [\lambda/(2Lk)]^{1/2} \quad (6)$$

The angular resolution of the ER-based method [22,44-47] is higher than the estimation (6), since one can measure even small reduction of visibility of the interference rings. An example of measured visible-range ER used for electron beam diagnostics in a storage ring is shown in Fig. 4.

The ER method is similar to the methods based on **transition** and **diffraction radiation** [47]. The ER seems more suitable for storage rings. However, with this method, one may need to know and to take into account extra sources of transverse magnetic field within a straight section, which bend particle trajectories and/or contribute to the angular distribution of the emitted radiation (correctors, quadrupoles). If this magnetic field is not known to a reasonable accuracy, the application of the ER-based technique may not be easy. On the other hand, one can use high-accuracy SR computation [16,45] to simulate emission from a straight section and judge both the electron beam emittance and the alignment of the electron beam optics in the straight section.

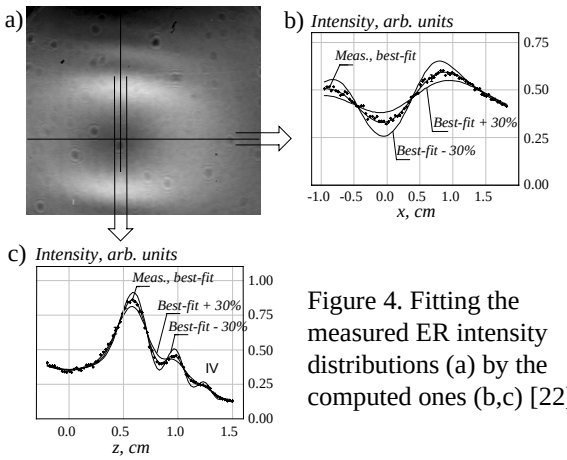

Figure 4. Fitting the measured ER intensity distributions (a) by the computed ones (b,c) [22].

4 FROM SIZE & DIVERGENCE TO EMITTANCE & ENERGY SPREAD

In order to deduce the beam emittance and the energy spread from the measured beam size(s), angular divergence(s), or their combinations (4), one can use the following well-known expressions for second-order central moments of particle distribution in the beam:

$$\begin{aligned} \sigma_x^2 &= \varepsilon_x \beta_x + (\sigma_E/E)^2 \eta^2, \\ \sigma_{x'}^2 &= \varepsilon_x (1+\alpha_x^2)/\beta_x + (\sigma_E/E)^2 \eta'^2, \\ M_{xx'} &= -\varepsilon_x \alpha_x + (\sigma_E/E)^2 \eta\eta', \end{aligned} \quad (7)$$

where β_x, α_x are the horizontal Twiss parameters, η, η' are the values of dispersion function and its derivative at the longitudinal position where the moments are measured; ε_x and σ_E/E are the horizontal emittance and relative energy spread respectively. The relations for vertical moments are obtained from Eqs. (7) assuming zero dispersion.

5 CONCLUSIONS

The optical diagnostics of relativistic particle beams benefits from the knowledge and exploitation of the wave-optical features of synchrotron radiation. A relatively large number of available optical methods allow choosing the most suitable one(s) for particular experimental conditions. To better estimate the emittance, a combination of methods, e.g. one imaging or interference method, and one projection method, can be used.

ACKNOWLEDGEMENTS

I would like to thank Dr. A.Snigirev, Dr. P.Elleaume, Dr. I.Snigireva, Dr. J-M.Filhol, Dr. R.Nagaoka (ESRF), and Dr. A.Anderson (MAX-Lab) for their precious help and discussions.

REFERENCES

[1] A.Hofmann and F.Meot, "Optical resolution of beam cross-section measurements by means of synchrotron radiation", Nucl. Instr. and Meth., 1982, vol.203, p.483.
[2] J.S.Mackay, "Electron beam profile, position systems and measurements on the Daresbury SRS", Proc. of EPAC-88; preprint DL/SCI/P591A, 1988.
[3] A.Ogata, "On optical resolution of beam size measurements by means of synchrotron radiation", Nucl. Instr. and Meth., 1991, vol.A301, p.596.
[4] K.Scheidt, "UV and visible light diagnostics for the ESRF storage ring", Proc. of EPAC-96, p.1621.
[5] Å.Andersson, M.Eriksson and O.Chubar, "Beam profile measurements with visible synchrotron light on MAX-II", Proc. of EPAC-96, p.1689.
[6] A.Snigirev, V.Kohn, I.Snigireva, B.Lengeler, "A compound refractive lens for focusing high-energy X-rays", Nature, 1996, vol.384, p.49.
[7] P.Elleaume, "Optimization of compound refractive lenses for X-rays", Nucl. Instr. and Meth., 1998, vol.A412, p.483.
[8] P.Elleaume, J. Synchrotron Rad., 1998, vol.5, p.1.
[9] B.Lengeler et. al., "Imaging by parabolic refractive lenses in the hard X-ray range", J. Synchrotron Rad., 1999, vol.6, p.1153.
[10] X-Ray Data Booklet, LBL PUB-490, 1986, edited by Douglas Vaughan, sect. 2-7.
[11] T.Weitkamp et. al., "Electron beam profile measurements with refractive X-ray lenses", these proceedings.
[12] P.Elleaume, private communication.
[13] P.Elleaume et. al., "Measuring beam size using X-ray pinhole camera", J. Synchrotron Rad., 1995, vol.2, p.209.
[14] Å.Andersson, "Electron beam profile measurements and emittance manipulation at the MAX-laboratory", Ph.D. thesis, Lund 1997.
[15] J.Bahrdt, "Wavefront propagation: design code for synchrotron radiation beamlines", Appl. Optics, 1997, vol.36(19), p.4367.
[16] O.Chubar, P.Elleaume, "Accurate and efficient computation of synchrotron radiation in the near field region", Proc. of EPAC-98, p.1177.
[17] N.V.Smolyakov, "Wave-optical properties of synchrotron radiation", Nucl. Instr. and Meth., 1998, vol.A405, p.235.
[18] O.Chubar, P.Elleaume and A.Snigirev, "Phase analysis and focusing of synchrotron radiation", Nucl. Instr. and Meth., 1999, vol.A435, p.495.
[19] O.Chubar, "Resolution improvement in beam profile measurements with synchrotron light", Proc. of IEEE PAC-93, vol.3, p.2510.
[20] T.Mitsuhashi, M.Katoh, "A construction of optical beam profile monitor for high brilliance configuration of the Photon Factory", Proc. of EPAC-96, p.1669.
[21] O.Chubar, "Transverse electron beam size measurements using the Lloyd's mirror scheme of synchrotron light interference", Proc. of IEEE PAC-95, p.2447.
[22] N.Artemiev, O.Chubar, A.Valentinov, "Electron beam diagnostics with visible synchrotron light on Siberia-1 ring", Proc. of EPAC-96, p.340.
[23] T.Mitsuhashi, "Spatial coherency of the synchrotron radiation at the visible light region and its application for the electron beam profile measurement", Proc. of IEEE PAC-97, p.766.
[24] N.V.Smolyakov, "Interference diagnostics for storage ring electron beam", Nucl. Instr. and Meth., 1998, vol.A405, p.229.
[25] S.Hiramatsu et. al., "Measurement of small beam size by the use of SR interferometer", Proc. of IEEE PAC-99, p.492.
[26] H.Hayano et. al., "Emittance measurement at KEK-ATF damping ring", Proc. of IEEE PAC-99, p.2143.
[27] A.Snigirev et. al., "On the possibilities of X-ray phase contrast micro-imaging by coherent high-energy synchrotron radiation", Rev. Sci. Instrum., 1995, vol.66(12), p.5486.
[28] A.Snigirev, "Coherent properties of the third generation synchrotron radiation sources: requirements to the optics", SPIE vol.2856, p.26.
[29] M.Born, E.Wolf, Principles of Optics, 4th ed., Pergamon Press, 1970.
[30] T.Shintake et.al., "Experiments of nanometer spot size monitor at FFTB using laser interferometry", Proc. of IEEE PAC-95, p.2444
[31] A.Snigirev, V.Kohn, I.Snigireva, "Fresnel diffraction by slits", in "ESRF Highlights 1996/1997", Nov.1997, p.91.
[32] E.Tarazona, P.Elleaume, "Emittance measurements at the ESRF", Rev. Sci. Instrum., 1995, vol.66(2), p.1874.
[33] B.X.Yang, A.H.Lumpkin, "Particle beam profiling techniques on the APS storage ring", AIP Proc., vol.390, 1997, p.491.
[34] B.X.Yang, A.H.Lumpkin, "Simultaneous measurement of electron beam size and divergence with an undulator", Proc. of IEEE PAC-99, p.2161.
[35] R.P.Walker, "Near-field effects in off-axis undulator radiation", Nucl. Instr. and Meth., 1988, vol.A267, p.537.
[36] E.Tarazona, P.Elleaume, "Measurement of the absolute energy and energy spread of the ESRF electron beam using undulator radiation", SRI-95, ANL, 17-20 October 1995.
[37] P.Elleaume, "Optical klystrons", Journal de Physique, 1983, vol.44, p.C1-332.
[38] R.Bossart et. al., "Observation of visible synchrotron radiation emitted by a high-energy proton beam at the edge of a magnetic field", Nucl. Instr. and Meth., 1979, vol.164(2), p.375
[39] M.M.Nikitin, A.F.Medvedyev, M.B.Moiseyev, "Synchrotron radiation from ends of straight-linear interval", IEEE Trans. Nucl. Sci., 1981, vol.NS-28, p.3130.
[40] Yu.A.Bashmakov, "Synchrotron radiation of electrons in the edge magnetic fields of storage rings", Rev. Sci. Instr., 1992, vol.63(1), p.343.
[41] O.Chubar, N.Smolyakov, "VUV range edge radiation in electron storage rings", J.Optics (Paris), 1993, vol.24(3), p.117.; also in Proc. of IEEE PAC-93, vol.2, p.1626.
[42] R.A.Bosch, "Long-wavelength edge radiation along a straight-section axis in an electron storage ring", Nucl. Instr. and Meth., 1997, vol.A386, p.525.
[43] C.Bovet, A.Burns, F.Meot, M.Placidi, E.Rossa, J. de Vries, "Synchrotron radiation interferences between small dipoles at LEP", Proc. of IEEE PAC-97, p.1987.
[44] O.Chubar, I.Nagornykh, Yu.Krylov, "Edge radiation based system for beam diagnostics on Siberia-1 electron storage ring", Proc. of EPAC-94, vol.2, p.1673.
[45] O.Chubar, "Precise computation of electron beam radiation in non-uniform magnetic fields as a tool for the beam diagnostics", Rev. Sci. Instrum., 1995, vol.66(2), p.1872.
[46] N.Smolyakov, A.Hiraya and H.Yoshida, "Edge radiation and electron beam diagnostics", Proc. of EPAC-98, p.1604.
[47] M.Ferianis, "Optical techniques in beam diagnostics", Proc. of EPAC-98, p.159.